ISSN 1330-3651 (Print), ISSN 1848-6339 (Online)
https://doi.org/10.17559/TV-20230121000255
Original scientific paper

A Sliding Mode Control Based Stabilization Method for Directional Rotary Steering Tool-Face

Cheng JI, Mengxiang DONG, Dezhou YU, Longhao LIU, Liancheng ZHANG*

Abstract: When the directional rotary steering system works in the state of maintaining the tool face angle, the use of PID control mode will lead to a large swing angle of the tool face angle of the directional rotary steering system. In order to reduce the swing amplitude of the tool face angle, based on the PID position control and the angle position error sliding mode control strategy, the exponential synovial control function is established. The simulation results show that the fast and accurate tool face angle tracking is achieved through the closed-loop control of the angle position. The paper provides an implementation method for the research of directional rotary steering system.

Keywords: permanent magnet synchronous motor; rotary steering system (RSS); sliding mode control; stabilized platform; tool face

1 INTRODUCTION

Rotary steering technology is a cutting-edge technology in the field of oil drilling. The working mode of RSS is to adjust the mandrel direction in real time, and drill smoothly according to the set drilling trajectory while drilling [1-2]. Compared with the traditional sliding guide tool, the rotary guide technology can simplify the drilling operation procedure, reduce the operation cost and improve the drilling operation accuracy; moreover, the borehole purification effect is better and the borehole trajectory accuracy is more accurate than the traditional sliding guide tool [3, 4]. During the drilling process, the bit can maintain the set inclination angle when the outer drill collar rotates, which can effectively avoid the phenomenon of supporting pressure on the well wall. Therefore, its displacement extension ability is more powerful, especially suitable for the operation requirements of special process wells such as ultra-deep wells, highly difficult directional wells, cluster wells and large displacement horizontal wells in complex oil and gas reservoirs. It greatly improves the operation efficiency and speed, reduces the operation cost and reduces the occurrence of drilling accidents [5]. However, it is a difficult problem to maintain the stability of the face angle of the rotary guide tool. Through PID control method, the swing angle of tool face angle can be controlled within ±7°.

2 LITERATURE REVIEW

At present, the rotary guidance technology mainly includes push type, directional type and compound type. Compared with other rotary steering systems, the directional rotary steering system is more suitable for complex downhole working environment since it does not depend on the geological conditions of the borehole wall. The smooth borehole wall reduces the risk of drill sticking [6].

1. Principle of directional rotary guidance system

The black ring in Fig. 1 is the drill collar section, and the inner ring is the mandrel section. When performing directional operation, the drill collar rotates clockwise at the speed ω, and the spindle drive rotates at the opposite direction in the same speed relative to the drill collar. At this time, the mandrel remains stationary relative to the earth.

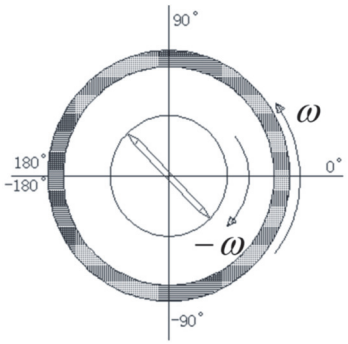

Figure 1 Schematic diagram of mandrel tracking principle

In Fig. 2, the front end of the mandrel is connected with the drill bit through the eccentric shaft. Since the drill bit no longer rotates relative to the earth, a stable platform is formed. Under the action of the eccentric shaft, the drill bit also remains stationary and points to a preset orientation to form a function similar to the bending screw, so as to realize the guiding operation. In order to form a stable platform and maintain the pointing stability of the tool-face angle, it is necessary to adjust the rotation speed of the mandrel in real time to make it track the drilling speed of the drill collar, and keep the tool face angle at the set reference tool face angle position while maintaining the same speed and opposite direction. The ultimate goal is to realize the real-time tracking of the mandrel angular position to the set reference angular position through the automatic control method [7-9].

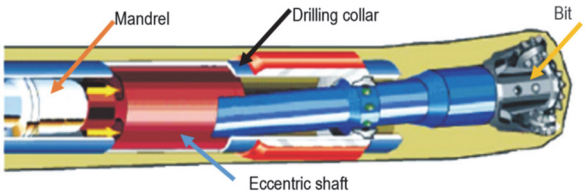

Figure 2 Structure diagram of directional rotary guide

The servo motor driving the spindle is a permanent magnet synchronous motor. In order to stabilize the tool face angle, it is necessary to realize the double closed-loop control of speed and tool face angle. The control method in the reference is to divide the mandrel tool face angle into four different intervals according to the circumferential 360 degree section, to judge the shortest path of the current tool face angle to the target tool face angle by the position

interval of the tool face angle, and to select the mandrel acceleration or deceleration according to the control strategy set in the program [10]. This control method is a PID double closed-loop control based on speed and rotor position. Although it can quickly track the tool face angle, when observing the control results, it will be found that the actual tool face angle of the mandrel swings on both sides of the preset tool face angle [11]. This will not only reduce the accuracy of directional operation, but also reduce the smoothness of shaft wall. Measured data of no-load experiment: when the target tool face angle is set at 180°, the actual value of the tool face angle is measured every 0.1 s and the measured value of the actual tool face angle is 171.5°-185.0°; the average value is 178°; and the variation range around the average value is about ± 7°.

3 RESEARCH METHODOLOGY

3.1 Control Principle

Sliding mode control is also called variable structure control, which is a special nonlinear control, and its nonlinearity is represented by the discontinuity of control. Sliding mode control is a control method with simple form but excellent control performance [12-13]. Compared with other control strategies, the difference is that the system structure is not fixed. It can be automatically adjusted according to the current state of the system in the dynamic process, so that the controlled system can move up and down with small amplitude and high frequency according to the predetermined state trajectory, which is called sliding mode. The sliding model can be designed according to the system and is independent of object parameters and disturbances [14-16]. Therefore, sliding mode control has the advantages of fast response, no system on-line identification, simple physical implementation and good robustness. Compared with the widely used PID linear control, the most significant advantage of sliding mode control is that it is insensitive to disturbance and can effectively avoid overshoot and undershoot in the process of PID control [17-19].

For a dynamic system with unknown disturbance, Eq. (1):

$$\begin{cases} \dot{x}_1 = x_2 \\ \dot{x}_2 = a(x_1, x_2) + b(x_1, x_2)u + d \\ y = x_1 \end{cases} \tag{1}$$

In Eq. (1), x stands for the state variable of the system; u stands for the control variable; y is the output function; a and b are two smooth uncertain state variables and is a bounded function of time. Assuming the output error [20, 21], $\Delta y = x_1^d - x_1 = e_1$, form the first-order sliding mode surface of exponential approach by Eq. (2), where $c > 0$:

$$s = \dot{e}_1 + ce_1 \tag{2}$$

It can be seen from Eq. (2) that when $t \to \infty$, the stable system converges $s(0)$, and the convergence speed depends on c.

Laypunov function defines Eq. (3):

$$V = \frac{1}{2}s^2 \tag{3}$$

Therefore, we get $\dot{V} = s\dot{s}$, and just make $\dot{V} < 0$, the system satisfies the convergence condition.

Considering that the ultimate purpose of the speed control of the directional rotary guide tool is to realize the tracking of the tool face angle of the spindle to the preset tool face angle, set the current tool face angle of the spindle as θ, the preset tool face angle as θ_{ref}, and the spindle speed as ω, u as the output of the controller, and then the state equation of the physical process is established as Eq. (4).

$$\begin{cases} x_1 = \theta - \theta_{\text{ref}} = e \\ x_2 = \dot{x}_1 = \dot{e} \end{cases} \tag{4}$$

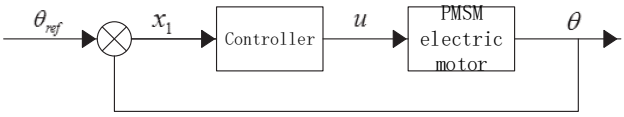

Figure 3 Diagram of tool face angle positioning system

Selecting a sliding surface approaching exponentially

$$s = cx_1 + x_2 = ce + \dot{e} \tag{5}$$

$$\begin{aligned} \dot{s} &= c\dot{e} + \ddot{e} = c\left(\dot{\theta} - \dot{\theta}_{ref}\right) + \ddot{\theta} - \ddot{\theta}_{\text{ref}} = c\dot{\theta} + \ddot{\theta} - c\dot{\theta}_{\text{ref}} \\ \theta &= \int_0^t \omega d\tau \to \dot{\theta} = \omega \to \ddot{\theta} = \frac{\mathrm{d}\omega}{\mathrm{d}t} \end{aligned} \tag{6}$$

Set the drill collar speed as a constant, 120 rpm, then $\omega_{\text{ref}} = 120\pi/30 = 4\pi(\text{rad/s})$

The voltage equation of permanent magnet synchronous motor (PMSM) in d_{q0} coordinate system is given by Eq. (7).

$$\begin{cases} u_d = Ri_d + L\dfrac{di_d}{dt} - p_n\omega Li_q \\ u_q = Ri_q + L\dfrac{di_q}{dt} + p_n\omega Li_d + p_n\omega\varphi_f \\ J\dfrac{d\omega}{dt} = \dfrac{3}{2}p_n\varphi_f i_q - T_L \end{cases} \tag{7}$$

We assume that the rotation speed of the drill collar is constant, and the rotation speed of the mandrel will shake due to the disturbance of the friction torque on the drill bit. Therefore [22], after combining Eq. (7) and adding interference $d(T_L)$ to Eq. (6), it becomes Eq. (8)

$$\dot{s} = c\dot{\theta} + \ddot{\theta} = c\dot{\theta} + \frac{1}{J}(u + d(T_L)) - 4c\pi \tag{8}$$

Eq. (9) is obtained according to the convergence condition of Laypunov function in Eq. (3):

$$\dot{V} = s\dot{s} = s\left(c\dot{\theta} + \frac{1}{J}(u + d(T_L)) - 4c\pi \right) \tag{9}$$

Only when

$$u = J(-c\dot{\theta} - \frac{1}{J}(ks + \eta \,\mathrm{sgn}(s)) + 4c\pi) \tag{10}$$

Substitute Eq. (10) into Eq. (9), where η is greater than the maximum amplitude of random interference, so as to obtain Eq. (11).

$$\dot{V} = \frac{1}{J}\left(-ks - \eta|s| + sd(T_L)\right) < -\frac{1}{J}ks^2 \tag{11}$$

Since the derivative of V is always less than 0, the Laypunov convergence condition is satisfied.

3.2 Establishment of Matlab Simulation Model

According to the above discussion and the derived Eq. (10), the simulation model is established by MATLAB. The model setting conditions are as follows: assuming that the drill collar rotates at a constant speed of 120 rpm, the reference angular velocity is $4\pi(\mathrm{rad/s})$, and the reference zero angle position of the drill collar will rotate according to the angular velocity $4\pi(\mathrm{rad/s})$. The spindle speed is the output speed of the permanent magnet synchronous motor, and the reference zero angle position of the spindle is the angular position of the rotor shaft of the permanent magnet synchronous motor. When the angular position of the permanent magnet synchronous motor is close to the angular position of the drill collar, the sliding mode controller will track the tool surface angle near the sliding mode surface. The function of sliding mode controller is established by Simulink, as shown in Fig. 4.

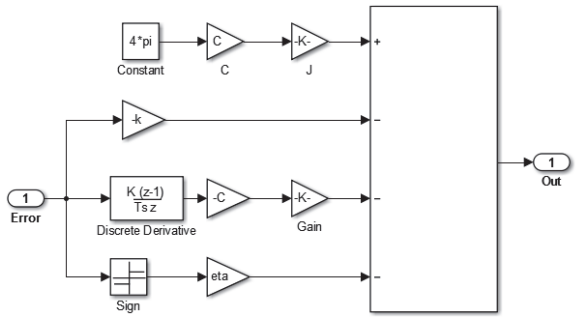

Figure 4 Design of sliding mode controller based on Simulink

The sliding mode controller in Eq. (10) includes three key parameters: c is the proportional gain coefficient of the speed error between the drill collar speed and the spindle speed, k is the proportional gain coefficient of the error between the preset tool face angle and the spindle tool face angle, and *eta* is the amplitude of the switching function. Different control parameters will have different effects on the control effect.

3.3 Comparison of Tool Face Angle Tracking Effect under Different Control Coefficients

Firstly, set the proportional gain c = 60 and switching function amplitude of the speed error *eta* = 40, adjust k, the proportional gain coefficient of the tool surface angle error from 200 to 500, and apply a random disturbance load with a peak to peak value of no more than 10 nm on the motor shaft, as shown in Fig. 5.

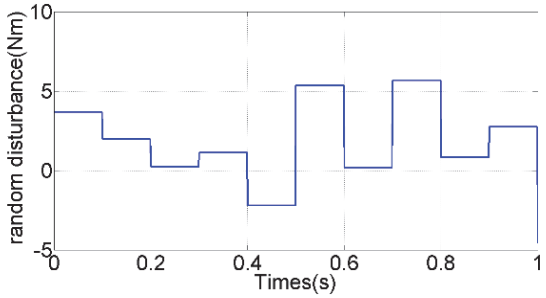

Figure 5 Random disturbance load

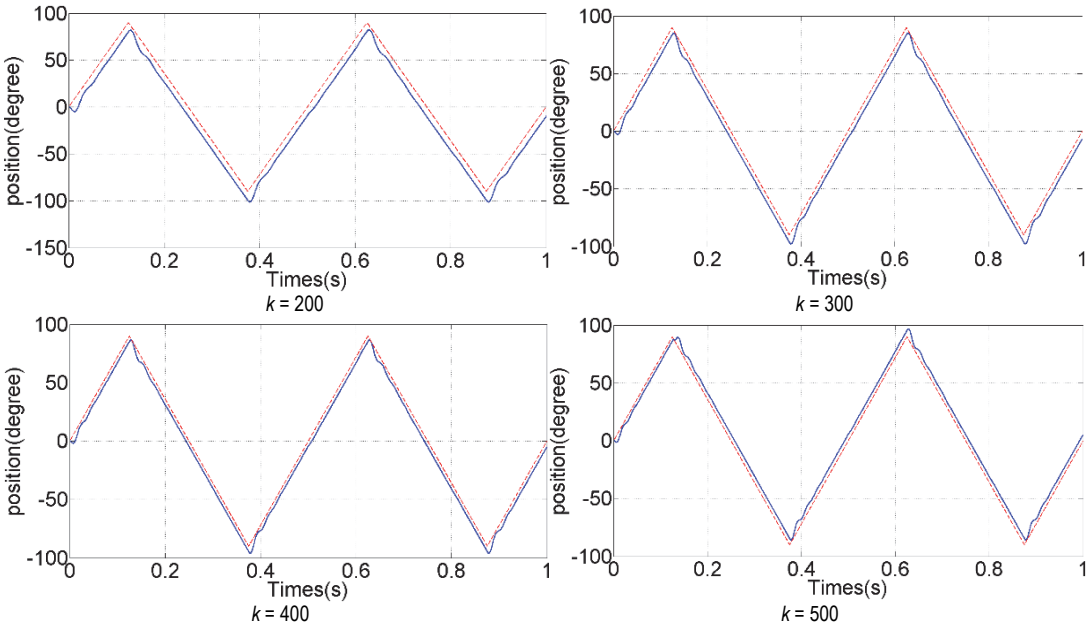

Figure 6 Influence of adjustment of k on control effect when c = 60 and *eta* = 40

The red dotted line in Fig. 6 is the standard curve of the drill collar rotating with 4π radians per second, and the blue solid line is the rotor shaft angle position curve of the permanent magnet synchronous motor after passing through the sliding mode controller (the same in Fig. 7 and 8). It can be seen from this set of curves that when k, the proportional gain coefficient of position error is 200, the error is always negative. With the increase of gain coefficient, the average error is closer to the sliding surface, but it will not pass through the sliding surface repeatedly. Moreover, when k, the gain coefficient is less than 400, the zero angle position of the mandrel always lags behind the set reference position. When *k* is over 500, except that it lags behind the reference position of the drill collar at the beginning of startup, the angular position of the mandrel has always been ahead of the drill collar. Therefore, by adjusting the proportional gain coefficient of the rotational speed error of the two, the output error can be close to the side where the sliding surface *s* is less than 0. When *k* is greater than 500, the output error will be close to the side where *s* is greater than 0.

In the second simulation, when the fixed switching function amplitude *eta* is equal to 40 and the holding position error proportional gain coefficient *k* is equal to 400, adjust the speed error proportional gain coefficient *c*, and the simulation results are shown in Fig. 7:

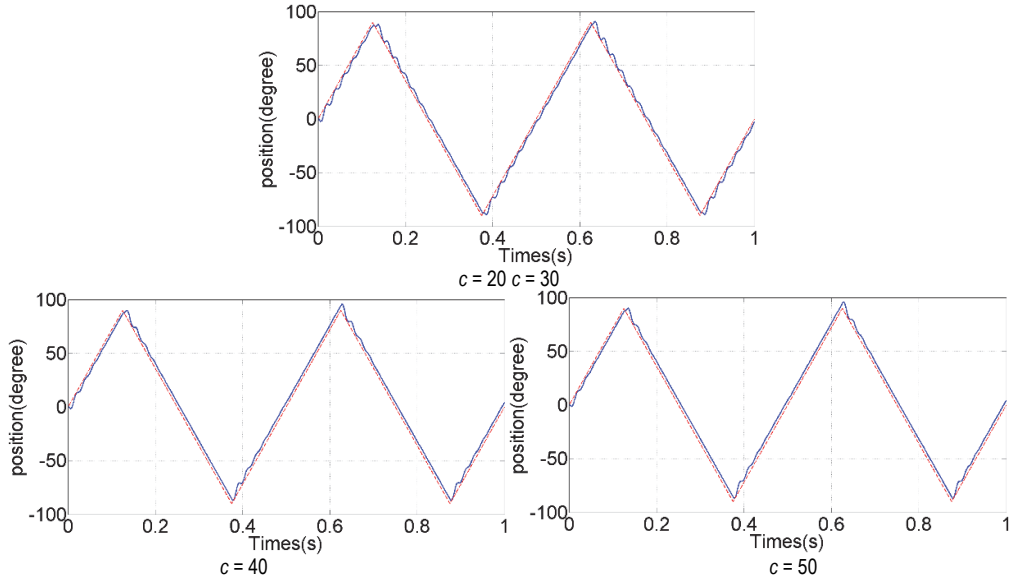

Figure 7 Influence of adjustment of *c* on control effect when *eta* = 40 and *k* = 600

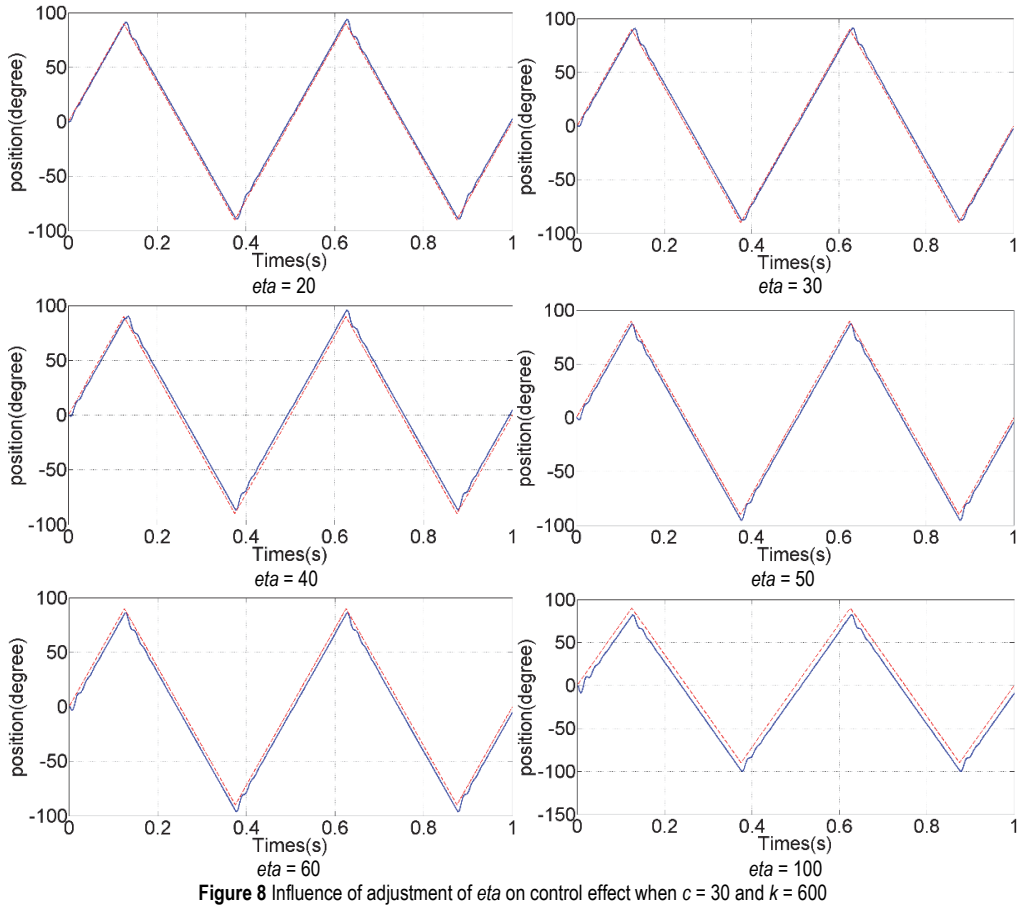

Figure 8 Influence of adjustment of *eta* on control effect when *c* = 30 and *k* = 600

It can be seen that when $c > 40$, the controller will repeatedly pass through the sliding mode surface to form chattering, rather than approaching only one side of the sliding mode surface. When $c = 50$, the spindle angle position will always be ahead of the drill collar angle position, and the controller starts to approach only on one side of the sliding surface when $s > 0$. Therefore, increasing the proportional gain coefficient of speed error can avoid the phenomenon that the output repeatedly passes through the sliding mode surface.

In the third simulation, keep the proportional gain of angular velocity error $c = 60$ and the proportional gain of angular position error $k = 600$ unchanged, and adjust the amplitude of switching function *eta* to obtain the simulation results shown in Fig. 8.

4 RESULTS AND DISCUSSION

By the previous analysis, when the position error proportional gain coefficient is between 300-400, the system output is closest to the sliding mode surface. When the set peak amplitude of random disturbance load is less than 10 and *eta*, the amplitude of switching function is greater than 50, the system output approaches one side along the sliding mode surface. The larger the value of speed error proportional gain coefficient *c*, the smaller the overall tracking error range of the system. Under this condition, the error curves of spindle angular position and reference angular position under different speed error proportional gain coefficients are measured, as shown in Fig. 9.

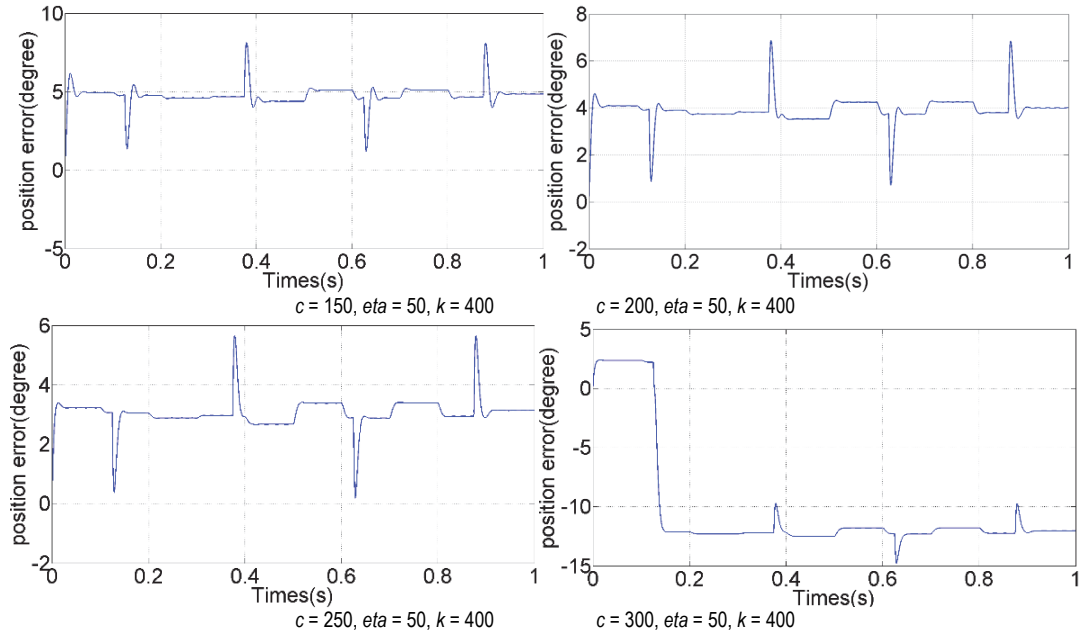

Figure 9 Error curve of spindle angular position and reference angular position under different speed error proportional gain coefficient

It can be seen from Fig. 9 that under this parameter combination, when the speed error proportional gain coefficient $c = 300$, the error is the smallest, only less than 2.5°, but there will be a process of passing through the sliding surface at the initial stage of startup. Moreover, with the further increase of the speed error proportional gain coefficient *c*, the error between the spindle angle position and the reference angle position will decrease, but the range of error reduction is very limited. Due to the automatic control system with too high gain coefficient, its anti-interference level will be reduced. In order to prevent this phenomenon, it is suggested that the gain coefficient *c* should be around 200.

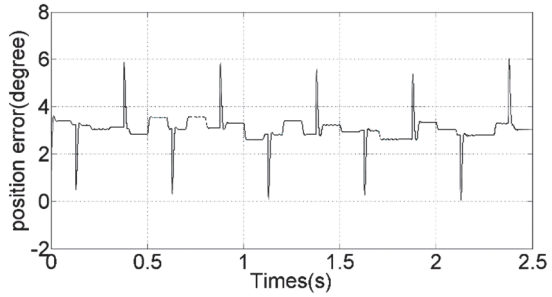

Figure 10 Tracking difference curve of mandrel angle position and drill collar angle position when $c = 230$, $eta = 50$, and $k = 400$

After many simulation tests, we finally select the set of parameters $c = 230$, $eta = 50$ and $k = 400$, and plot the dynamic error curves of the preset tool face angle and the actual tool face angle and their tracking curves shown in Fig. 10 and Fig. 11.

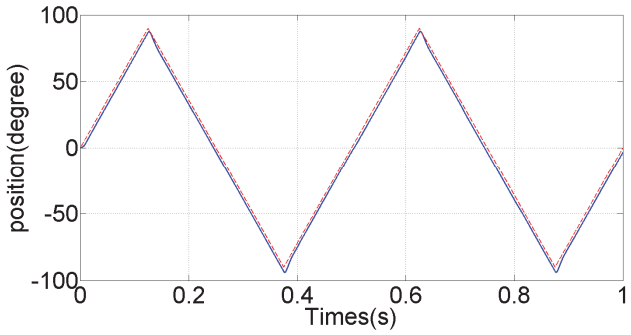

Figure 11 Tracking curve of mandrel angle position and drill collar angle position when $c = 230$, $eta = 50$, and $k = 400$

It can be seen from the angular position difference curve in Fig. 10 that the angular position of the mandrel is always about 3° ahead of the reference angular position of the drill collar. In the actual control program, the central position can be compensated to zero by setting the

compensation coefficient constant. Under the sliding mode controller with this parameter, it can be seen that the designed sliding mode controller has very good robustness. The spindle angular position swings left and right around the reference angular position of the drill collar, and the maximum angle on one side is no more than 3°. The angular position tracking accuracy is improved to 0.8%, and the performance is obviously better than the single speed error PID control. Fig. 11 shows the tracking state of mandrel angular position to drill collar reference angular position under this set of parameters.

5 CONCLUSION

In this paper, the stability of the steering angle of the tool deployment system is studied. The tool face angle stabilization strategy of the existing directional rotary guidance system is a PID linear control method based on the spindle speed. This control method will lead to a large reciprocating swing of the spindle tool face angle near the set tool face angle, and the experimental results show that the swing amplitude is between ±7° under no-load condition. In order to reduce the swing amplitude of the tool face angle, based on the PID position control and the angle position error sliding mode control strategy, the exponential synovial control function is established. Under the joint action of the two control methods, the swing amplitude of the mandrel tool face angle is effectively reduced to ±2.5°. Matlab simulation proves that this control method is feasible theoretically, which provides a feasible theoretical method for the development of directional rotary guidance tool and improving control accuracy. Although the sliding mode control based on angular position error can effectively reduce the swing amplitude of the tool face angle of the eccentric shaft, this control method requires error feedback before the controller can reflect the action, and the time delay of this feedback control leads to the error that cannot be further reduced. However, it still has important research value for the development of directional rotary guidance system.

Acknowlegement

The paper was funded by the North China Institute of Aerospace Technology doctoral research fund project (BKY-2021-19).

6 REFERENCE

[1] Epikhin, A., Zhironkin, V., Szurgacz, D., & Trzop, K. (2021). Method for determining the loads on the deflection module of the push-the-bit rotary steerable system. *IOP Conference Series: Earth and Environmental Science*, *684*(1), 012001. https://doi.org/10.1088/1755-1315/684/1/012001

[2] Zafarian, H., Ameri, M., & Vaghasloo, Y. A. (2021). Error reduction of tracking planned trajectory in a thin oil layer drilling using smart rotary steerable system. *Journal of Petroleum Science and Engineering*, *196*, 107668. https://doi.org/10.1016/j.petrol.2020.107668

[3] Zhironkin, V., Epikhin, A., Novoseltsev, D., & Cehlár, M. (2020). Determination of the Loads on the Steering Module of the Push-the-Bit Rotary Steerable System in the Context of Its Reliability. *Acta Montanistica Slovaca*, *25*(3). https://doi.org/10.46544/AMS.v25i3.11

[4] Andrade, C. P., Saavedra, J. L., Tunkiel, A., & Sui, D. (2021). Rotary steerable systems: mathematical modeling and their case study. *Journal of Petroleum Exploration and Production Technology*, *11*, 2743-2761. https://doi.org/10.1007/s13202-021-01182-6

[5] Xinjun, G. & Jing, L. (2014). Research on application of steering drilling technologies in shale gas development. *Procedia Engineering*, *73*, 269-275. https://doi.org/10.1016/j.proeng.2014.06.198

[6] Huang, W., Wang, G., & Gao, D. (2021). A method for predicting the build-up rate of "push-the-bit" rotary steering system. *Natural Gas Industry B*, *8*(6), 622-627. https://doi.org/10.1016/j.ngib.2021.11.010

[7] Demirer, N., Zalluhoglu, U., Marck, J., Darbe, R., & Morari, M. (2019, July). Autonomous directional drilling with rotary steerable systems. *2019 American Control Conference (ACC)*, 5203-5208. https://doi.org/10.23919/ACC.2019.8814644

[8] Kamel, M. A., Elkatatny, S., Mysorewala, M. F., Al-Majed, A., & Elshafei, M. (2018). Adaptive and real-time optimal control of stick–slip and bit wear in autonomous rotary steerable drilling. *Journal of Energy Resources Technology*, *140*(3). https://doi.org/10.1115/1.4038131

[9] Sheng, L., Niu, Y., Wang, W., Gao, M., Geng, Y., & Zhou, D. (2021). Estimation of Toolface for dynamic point-the-bit rotary steerable systems via nonlinear polynomial filtering. *IEEE Transactions on Industrial Electronics*, *69*(7), 7192-7201. https://doi.org/10.1109/TIE.2021.3097601

[10] Li, Z., Shi, S., & Zhang, C. (2018). Active Return Control Strategy of Electric Power Steering System Based on Disturbance Observer. *Journal of Engineering Science & Technology Review*, *11*(3). https://doi.org/10.25103/jestr.113.09

[11] Alturbeh, H., Whidborne, J. F., Luk, P., & Bayliss, M. (2019). Modelling and control of the roll-stabilised control unit of a rotary steerable system directional drilling tool. *The Journal of Engineering*, *2019*(17), 4555-4559. https://doi.org/10.1049/joe.2018.8211

[12] Ding, S., Park, J. H., & Chen, C. C. (2020). Second-order sliding mode controller design with output constraint. *Automatica*, *112*, 108704. https://doi.org/10.1016/j.automatica.2019.108704

[13] Atay, S., Bryant, M., & Buckner, G. (2021). Control and control allocation for bimodal, rotary wing, rolling–flying vehicles. *Journal of Mechanisms and Robotics*, *13*(5). https://doi.org/10.1115/1.4050998

[14] Oubellil, R., Voda, A., Boudaoud, M., & Régnier, S. (2019). Mixed stepping/scanning mode control of stick-slip SEM-integrated nano-robotic systems. *Sensors and Actuators A: Physical*, *285*, 258-268. https://doi.org/10.1016/j.sna.2018.08.042

[15] Thanh, H. L. N. N. & Hong, S. K. (2018). Quadcopter robust adaptive second order sliding mode control based on PID sliding surface. *IEEE Access*, *6*, 66850-66860. https://doi.org/10.1109/ACCESS.2018.2877795

[16] Rahmat, M. F., Othman, S. M., Rozali, S. M., & Has, Z. (2018, October). Optimization of Modified Sliding Mode Control for an Electro-Hydraulic Actuator System with Mismatched Disturbance. *2018 5th International Conference on Electrical Engineering, Computer Science and Informatics (EECSI)*, 1-6. https://doi.org/10.1109/EECSI.2018.8752807

[17] Behera, A. K., Bandyopadhyay, B., & Yu, X. (2018). Periodic event-triggered sliding mode control. *Automatica*, *96*, 61-72. https://doi.org/10.1016/j.automatica.2018.06.035

[18] Van, M., Mavrovouniotis, M., & Ge, S. S. (2018). An adaptive backstepping nonsingular fast terminal sliding mode control for robust fault tolerant control of robot

manipulators. *IEEE Transactions on Systems, Man, and Cybernetics: Systems*, *49*(7), 1448-1458. https://doi.org/10.1109/TSMC.2017.2782246

[19] Haghighi, D. A. & Mobayen, S. (2018). Design of an adaptive super-twisting decoupled terminal sliding mode control scheme for a class of fourth-order systems. *ISA transactions*, *75*, 216-225. https://doi.org/10.1016/j.isatra.2018.02.006

[20] Riani, A., Madani, T., Benallegue, A., & Djouani, K. (2018). Adaptive integral terminal sliding mode control for upper-limb rehabilitation exoskeleton. *Control Engineering Practice*, *75*, 108-117. https://doi.org/10.1016/j.conengprac.2018.02.013

[21] Jahanshahi, H., Yousefpour, A., Munoz-Pacheco, J. M., Moroz, I., Wei, Z., & Castillo, O. (2020). A new multi-stable fractional-order four-dimensional system with self-excited and hidden chaotic attractors: Dynamic analysis and adaptive synchronization using a novel fuzzy adaptive sliding mode control method. *Applied Soft Computing*, *87*, 105943. https://doi.org/10.1016/j.asoc.2019.105943

[22] Cucuzzella, M., Lazzari, R., Trip, S., Rosti, S., Sandroni, C., & Ferrara, A. (2018). Sliding mode voltage control of boost converters in DC microgrids. *Control Engineering Practice*, *73*, 161-170. https://doi.org/10.1016/j.conengprac.2018.01.009

Contact information:

Cheng JI
North China Institute of Aerospace Engineering

Mengxiang DONG
State Grid Qinghai Electric Power Company Ultra High Voltage Company

Dezhou YU
CNPC Engineering Technology R&D Company Limited

Longhao LIU
Zhangjiakou Branch of State Power Investment Group Hebei Electric Power Co., Ltd.

Liancheng ZHANG
(Corresponding author)
1. North China Institute of Aerospace Engineering
2. Hebei Electric Vehicle Charging Technology Innovation Center
E-mail: wanshu5604@163.com